PERSPECTIVE

High efficiency III–V nanowire solar cells: the road ahead

Paola Prete* and **Nico Lovergine**

Department of Innovation Engineering, University of Salento, Via Monteroni, I-73100 Lecce, Italy

* Author to whom any correspondence should be addressed.

E-mail: paola.prete@unisalento.it

Keywords: nanowire solar cells, intermediate-band gap semiconductors, dilute nitride III–V compounds, multiple-band absorption, self-assembly technology, MOVPE, MBE

OPEN ACCESS

RECEIVED
27 July 2025

REVISED
3 September 2025

ACCEPTED FOR PUBLICATION
6 October 2025

PUBLISHED
24 October 2025

Original content from this work may be used under the terms of the Creative Commons Attribution 4.0 licence.

Any further distribution of this work must maintain attribution to the author(s) and the title of the work, journal citation and DOI.

Abstract

Solar cells (SCs) based on dense arrays of III–V nanowires have long been considered strong candidates for the fabrication of stable, high power conversion efficiency (PCE) photovoltaic devices at reduced costs. Over the last two decades intense research has been devoted worldwide to the field; however, the nanowire SCs (NWSCs) reported so far in the literature have not confirmed theoretical expectations, their PCE figures remaining well below 18% under 1-sun illumination. The present work proposes an innovative strategy to overcome this limitation, i.e. through the use of intermediate-band gap semiconductors (IBGSs), namely GaNAs and related dilute-nitride III–V (III-N-V) compounds, as nanowire absorbing materials in substitution of the most common GaAs and InP. This allows us to combine the multi-band absorption functionality of IBGSs with the advantages associated with NWSCs, i.e. the super-absorptive properties of dense nanowire arrays and reduced volumes of active materials. Very high PCEs are expected for such nanowire-based intermediate band SCs. However, their practical realization requires suitably designed core-multishell radial junction nanowire heterostructures; an example of a perspective nano-device architectures is described herein. The potential and possible limitations/challenges facing current nanowire self-assembly technologies for the fabrication of the proposed III-N-V based nanowire IBSCs are discussed.

1. Introduction

As the use of conventional fossil-based fuels for energy production appears nowadays to be the major source responsible for global warming, the technological availability of alternative clean and renewable energy sources has become more critical than ever. Among other renewable energy sources, solar (especially photovoltaic (PV)) sources stand out as a viable solution to address the growing world energy demand, while mitigating environmental effects and contributing to secure some of the 2030 Sustainable Development Goals prescribed by the United Nations [1, 2]. The current PV market for ground-based applications is largely dominated by bulk (crystalline and polycrystalline) silicon (Si) and, to a lesser extent, inorganic thin films (e.g. based on CdTe [3] and Cu(In,Ga)Se_2 [4]) single-junction solar cells (SCs). Potentials for further improvements of the power conversion efficiency (PCE) figures of such cells are, however, limited by fundamental physics mechanisms [5, 6] and technological constraints [7]. To overcome these limitations, researchers in the field have been focusing on new materials/device concepts and novel mechanisms of solar power conversion into electricity (e.g. multiband absorption, hot carrier excitations, up/down conversion, etc), with the aim to maximize both the PCE and the long-term stability of perspective SCs, while reducing their production costs [8]. A promising strategy to achieve such objectives goes through the development of nanostructured SCs, in which reduced volumes of nanocrystalline semiconducting materials are employed, enabling researchers to exploit novel and more efficient physical mechanisms for solar power absorption and conversion into electricity at lower costs.

Within this approach, nanowires of III–V compound semiconductors are considered promising nanosystems for the fabrication of next generation high-efficiency and low-cost SCs; furthermore, they are also strong and well proven candidates for novel and efficient light-emitting devices [9, 10], fast and

© 2025 The Author(s). Published by IOP Publishing Ltd

polarization-sensitive photo-detectors [11–13], negative differential resistance devices [14], and a platform for future quantum technology devices, e.g. nanoscale single-photon sources [15]. Taken together, such potential has attracted a steady research interest worldwide in nanowire physics and technology since the early 2000's. Intense research efforts have been devoted, in particular, to the development of dense arrays of free-standing III–V nanowires, and early examples of GaAs [16] and InP [17] based nanowire SCs (NWSCs) had already been reported back in 2009. Since then, studies in the field have led to a rapid increase in their PCE figures, giving rise to a widespread enthusiasm for NWSCs. However, the III–V based NWSCs reported so far in the literature have not confirmed their initial theoretical expectations, with their PCE figures remaining well below 18% under 1-sun illumination. Furthermore, no substantial improvements in their PCE figures have been reported since 2016, despite the large research efforts devoted to the topic worldwide.

In this paper, we propose a new generation of NWSCs, based on the combination of the nanowire array SC architecture with intermediate bandgap semiconductors (IBGSs) as solar photon absorbing materials, namely the highly mismatched dilute-nitride III–V (III–N–V) compounds. We claim that such nanowire intermediate band SCs (IBSCs) promise to overcome the limitations encountered so far in conventional NWSCs. The perspective architectures of such novel nanowire-based IBSCs are described here, and the potential and possible limitations/challenges facing current self-assembly technologies for the synthesis of III–N–V based nanowires are discussed.

2. III–V NWSCs: the state-of-the-art

Nanowire technology. The synthesis of semiconductor nanowires relies on the intense research and development activities performed worldwide over the last two decades. III–V nanowires, in the form of dense ensembles (arrays) vertically standing on a single-crystalline substrate (Si, GaAs, InP, etc), are (mostly) obtained by molecular beam epitaxy (MBE) and metalorganic vapor phase epitaxy (MOVPE) technologies, through suitable combinations of bottom-up (so-called self-assembly) methods and conventional growth. The major features of these methods are that they allow fairly precise and reproducible control over the nanowire size, shape, density, material composition and/or intentional doping either along the nanowire length or in the lateral (radial) direction. Self-assembly of free-standing nanowires is obtained by (i) metal-catalyst assisted growth, (ii) self-catalyzed growth, or (iii) selective-area epitaxy (SAE). The first two methods rely on the vapor–liquid–solid (VLS) mechanism [18, 19] in which a metal (e.g. Au or Sn for metal-catalyzed growth, Ga or In for self-catalyzed growth) nanoparticle in contact with the substrate reacts and forms a liquid alloy with one or more group-III metal elements supplied from the vapor phase (the vapor). The NP forms then a supersaturated liquid alloy droplet (the liquid); upon group-V element supply, solid state precipitation (nucleation) and the subsequent growth of a crystalline III–V compound nanowire (the solid) at the NP/substrate interface is obtained; [111]-oriented nanowires are preferentially grown by these methods. The use of (111)-oriented substrates allows then to obtain vertically-standing nanowires with high yields [20]. Changing the vapor composition/doping during the VLS process allows for the growth of axially-modulated nanowire heterostructures; in particular, low background [21] as well as tunable and high doping levels [22] have been demonstrated for III–V nanowires. Radial growth of semiconducting compounds around a central (VLS-grown) nanowire core allows one to then obtain core-(multi)shell radial heterostructures, a process obtained by inhibiting the catalyst-assisted axial-growth process in favor of a conventional (i.e. vapor–solid (VS)) growth [23]; in MBE and MOVPE this change of growth regime is achieved by changing the growth temperature. The SAE process avoids the use of a metal catalyst, relying instead on the VS growth of the III–V compound within the openings of nano-patterned thin-film dielectric (SiO_2, SiN_x) masks fabricated on the substrate; for GaAs nanowires, high temperatures (750 °C) and As-reach vapor conditions ensure (i) selective growth (i.e. within the openings but not on the mask) and (ii) large growth rate anisotropy of the nano-crystal. Micron-long nanowires can then be (vertically) assembled along the [111] substrate direction, while keeping their diameter relatively small (within a few hundred nm). As for the other methods above, radial heterostructures can be achieved by changing the vapor composition during nanowire growth. Several reviews can be found in the literature on the self-assembly of III–V nanowires by MBE and MOVPE technology.

NWSC performance vs device architecture. The actual potentials of III–V NWSCs against conventional (planar) devices can be readily evaluated by considering their maximum PCE figures, as obtained from theoretical calculations. Indeed, the PCEs of single-junction NWSCs exceed that of planar SCs: efficiencies of ~42% and ~32.5% have been calculated under AM 1.5 illumination for a bandgap of 1.43 eV and 1.34 eV respectively, against the 31–33% figures expected for planar devices with the same bandgap

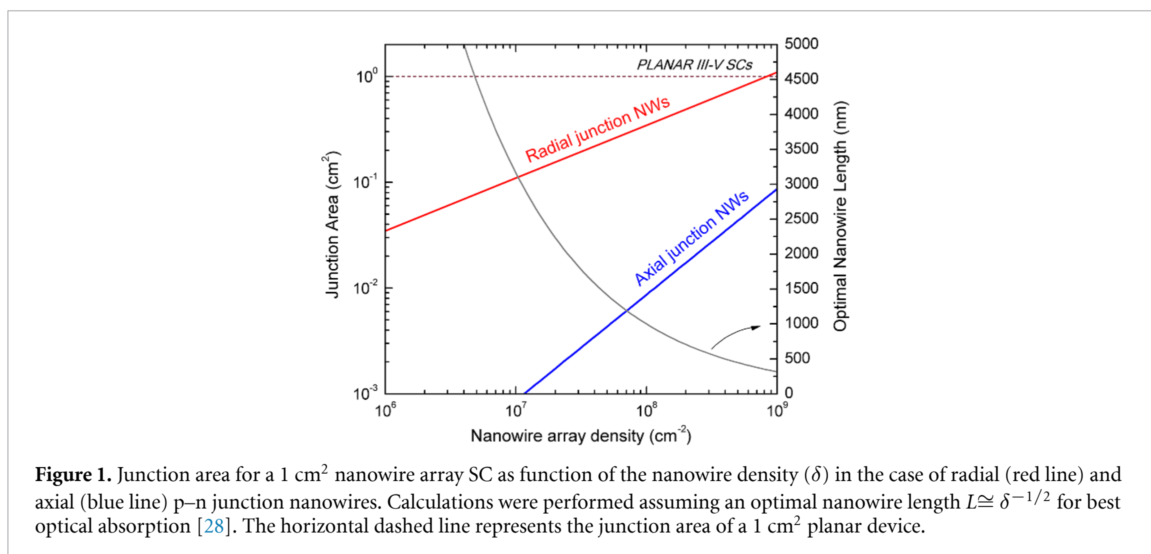

Figure 1. Junction area for a 1 cm^2 nanowire array SC as function of the nanowire density (δ) in the case of radial (red line) and axial (blue line) p–n junction nanowires. Calculations were performed assuming an optimal nanowire length $L \cong \delta^{-1/2}$ for best optical absorption [28]. The horizontal dashed line represents the junction area of a 1 cm^2 planar device.

[6]. Such theoretical performance relates to the peculiar interaction of light with nanowires, which has no analogue in the case of planar thin films (see next section).

Since the first demonstration of GaAs-based NWSCs in 2009 [16] it was clear that the nanowire large surface-to-volume ratios would, however, make NWSCs very sensitive to recombination/trapping of photo-generated carriers at nanowire surface states, leading to reduced short-circuit currents (j_{sc}) and PCEs. This mechanism is especially relevant for GaAs-based nanowires because of the large surface recombination velocity (SRV $\sim 10^5$ cm s^{-1}) of GaAs, but remains non-negligible even for InP-based nanowires, despite the fact that the carrier SRV of InP is three orders of magnitude lower [24]. Passivation of the nanowire by overgrowing the core (active) nanowire material with a wider bandgap III–V alloy shell has been shown to be effective in reducing/suppressing this effect. Indeed, a record 15.3% PCE figure was reported in 2016 by Åberg *et al* [25] for an AlGaAs-shell passivated axial (i.e. along the nanowire length) p–n junction GaAs NWSC. Overgrowth of radial p–n junction GaAs nanowires by InGaP shells was shown to increase the cell efficiency by up to 6.63% [26], indicating that proper passivation of surface states remains also important for the radial junction nanowire geometry.

Over the last 15 years, most researches in the field have focused on the implementation of SCs based on axial p–n (or p–i–n) junction nanowire geometry, while comparatively fewer studies have been reported on radial p–n junction nanowires [16, 26], as it is commonly believed that separation, transport and subsequent collection of photo-generated charge carriers along the length of an axial p–n junction nanowire would be less prone to nanowire surface/interface state recombination as it would be for a radial p–n junction, a consideration apparently supported by the lower PCE figures shown by radial junction NWSCs with respect to axial ones. This gives room to further speculation about the advantages of axial over radial junctions in NWSCs, a major difference residing in the larger junction areas of the latter [27]. Simple calculations of the junction areas for arrays of NWSCs as a function of nanowire densities—and supposing optimal nanowire length (for best light absorption) [28]—demonstrate that junction areas lower than that of a planar single-junction III–V SC can be estimated for both nanowire junction geometries (see figure 1); noteworthy, the PCE figures reported so far for NWSCs remain well below those of equivalent planar III–V SCs, suggesting that the device junction area alone may not be a solid argument for choosing between axial and radial junction geometry.

A modified National Renewable Energy Laboratory (NREL) chart of SCs record PCE, which includes NWSCs, was reported by Goktas *et al* [29], showing that the race for higher efficiencies in single-junction NWSCs had already reached its end by 2016. To further raise their PCE figures, more complex heterostructured nanowires have been proposed in an attempt to mimic the multi-junction architecture of planar III–V tandem SCs: a mixed axial/radial multi-band nanowire-based tandem device architecture was proposed by Wang *et al* [30], despite such nanowire structures being not easy to fabricate by self-assembly; a simpler InGaP/InP tandem axial-junction NWSC was also recently reported [31], although it achieved a mere PCE of 3.6%. Yao *et al* [32] reported a PCE of 11.4% for tandem SCs obtained by un-passivated axial p–i–n junction GaAs nanowires grown on a planar Si p–n junction, a striking result considering that the underlying Si SC was not optimized and that the GaAs bandgap is far from the optimal value (1.7–1.8 eV) requested for a III–V/Si tandem SCs. The latter issue could be sorted out by opting for As-rich GaAsP with an alloy composition matching the required spectral range [33]; however,

no further attempts were reported on tandem NWSCs. Finally, III–V core − shell nanowires have been recently reported for applications to hot-carrier NWSCs [34, 35], aiming for a 67% PCE under 1-sun irradiation conditions.

Light management. As the nanowire dimensions are comparable to or smaller than the solar photon wavelengths, the common ray-optics assumptions for analyzing conventional thin-films are no longer applicable. In this case, wave-optics modeling shall be adopted to correctly describe the interaction of the electromagnetic (e.m.) field with the nanowires.

Theoretical and experimental studies on this topic have shown that dense arrays of core–shell nanowires behave as super-absorptive media, as a result of different and concurrent light interaction mechanisms: (i) nano-antenna effect, (ii) wave-guiding, and (iii) multiple scattering/trapping of light. The first of these mechanisms is ascribed to the nanowires being able to absorb light from areas much larger than their own size; cross sectional areas around 1×10^6 nm^2 for photon absorption near the fundamental bandgap have been estimated by Krogstrup *et al* [36] for a 380 nm diameter single GaAs nanowire, corresponding to a light concentration enhancement of $\sim$12× with respect to a planar thin film: as a result, a short-circuit photocurrent of 180 mA cm^{-2} has been experimentally estimated for a single core–shell p–n junction GaAs nanowire diode, which is more than one order of magnitude higher than that predicted from the Lambert–Beer law. An estimated PCE $\sim$40%, i.e. well beyond the Shockley–Queisser limit for a single-junction GaAs SC (28.8% [6]), was then reported for such a single-nanowire device. Finite difference time-domain (FDTD) analyses carried out on dense arrays of vertically standing uniform nanowires have further shown that the light absorption enhancement depends on the number and strength of e.m. modes within the nanowires, which in turn depends on the nanowire size (diameter, length) and areal density (δ), the highest light absorption obtained for arrays in which the nanowire length (L) matches the average nanowire distance (i.e. $L {\sim} \delta^{-1/2}$) [28]. Notably, efficient absorption of solar photons would thus require nanowire densities in the 10^8 cm^{-2} range or less, corresponding to very low amounts of material [37].

A second mechanism leading to large optical absorption enhancement arises from wave-guiding of the incident light within core–shell nanowires, where the absorbing core material is surrounded by a wider bandgap (i.e. lower refractive index) shell material. We recently demonstrated that GaAs–AlGaAs core–shell nanowires show strong enhancement of the near band-edge (excitonic) GaAs optical absorption, depending on the actual thickness of AlGaAs shells [37]. Analyses of photo-reflectance spectra of dense arrays of GaAs–AlGaAs nanowires with respect to a reference planar structure showed for the first time a significant enhancement (up to 30×) of the GaAs band-edge optical absorption. Values of the integrated Lorentzian moduli of the exciton resonances, normalized to the nanowire array GaAs core volume relative to that of a planar layer having a thickness equal to the nanowire height, allowed to obtain a first ever estimate of the GaAs near band-edge absorption enhancement factor: values in the range 22–190 were obtained in [37] depending on the actual AlGaAs shell thickness. FDTD simulations show that for a very thin shell thickness the absorption enhancement remains relatively small, as in this case the guided-modes tend to be squeezed out of the GaAs core and onto the core−shell nanowire surface (air modes) [38, 39]; instead, increasing the shell thickness localizes the light more and more into the nanowires (dielectric resonance modes) allowing for higher absorption efficiencies. AlGaAs shell thickness of $\sim$40 nm gives rise to the best optical absorption in dense ($\delta \sim 10^8$ cm^{-2}) nanowire arrays [37].

The combination of nano-antenna and light wave-guiding effects leads to a concentration of the incident solar radiation within the nanowires. Surprisingly, very few FDTD studies have been performed to date to support the design and fabrication of core–shell NWSCs, despite the fact that most NWSCs utilize a wide bandgap shell for passivation purposes. Inherent light concentration in the order of 200 or more can be expected under optimized conditions. As both the j_{sc} and open-circuit voltage (V_{oc}) values of an SC increase with light concentration, correspondingly large theoretical PCEs can be predicted for NWSCs [40, 41].

3. Nanowire-based intermediate bandgap SCs

An innovative approach to improve the PCE of NWSCs consists of combining the nanowire architecture with the concept of intermediate-band SCs (IBSCs), namely by utilizing dilute nitride III-arsenide (III–N–V) compound semiconductors as the solar photon absorbing material [42].

IBSCs represent a well-known type of multi-band absorption single-junction devices, potentially able to reach PCEs well beyond the thermodynamic limiting values for single-bandgap absorption cells [6]. The concept of IBSCs was first proposed by Luque and Martì [43] and refers to the introduction of a

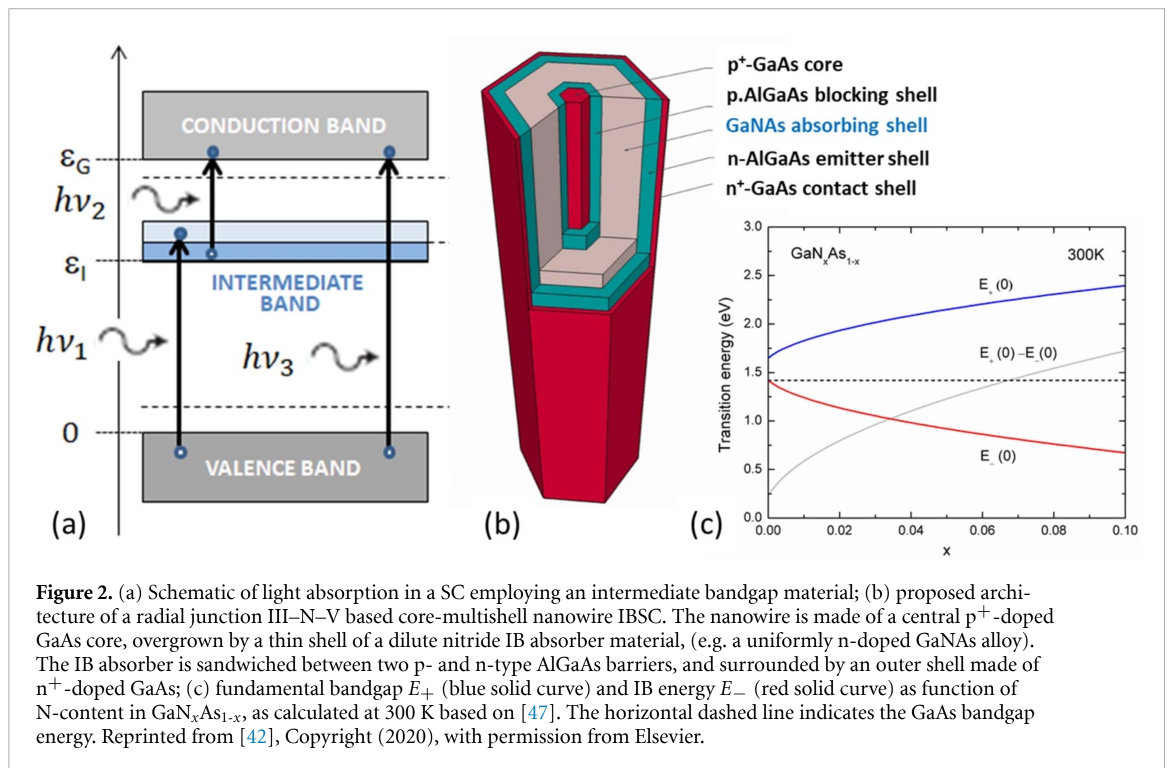

Figure 2. (a) Schematic of light absorption in a SC employing an intermediate bandgap material; (b) proposed architecture of a radial junction III–N–V based core-multishell nanowire IBSC. The nanowire is made of a central p^+-doped GaAs core, overgrown by a thin shell of a dilute nitride IB absorber material, (e.g. a uniformly n-doped GaNAs alloy). The IB absorber is sandwiched between two p- and n-type AlGaAs barriers, and surrounded by an outer shell made of n^+-doped GaAs; (c) fundamental bandgap E_+ (blue solid curve) and IB energy E_- (red solid curve) as function of N-content in GaN_xAs_{1-x}, as calculated at 300 K based on [47]. The horizontal dashed line indicates the GaAs bandgap energy. Reprinted from [42], Copyright (2020), with permission from Elsevier.

relatively narrow band (the so-called intermediate band IB) of discrete states within the fundamental gap of the semiconductor constituting the SC active material, such that, in addition to radiative transitions between the semiconductor valence (VB) and conduction (CB) bands, solar photon absorption occurs also through electronic transitions (i) from the VB to the IB, and (ii) from the IB to the CB (see figure 2(a)). To this end, the IB must be half-filled with electrons to provide both empty and occupied states, allowing for sufficient two-step photon absorption (TSPA) rates [44], and the IB states must be electrically isolated from the charge collecting contacts, ensuring that the SC operating voltage (V_{oc}) is solely determined by the fundamental (larger) bandgap of the IB material [43]. Recent simulations of planar IBSC structures based on a GaNAs absorbing layer have shown that the GaNAs alloy must be n-type doped around 10^{17}–10^{18} cm^{-3} to achieve large TSPA rates and thus good IBSC performance [45].

III–N–V alloys represent a well-known class of IBGSs [42]. Figure 2(c) shows the variation of the GaNAs fundamental bandgap (so called E_+) and the IB one (E_-) as a function of N-content in the alloy: as the N concentration increases, the E_+ bandgap rapidly increases above that of GaAs (and towards the visible light region), while the E_-one shifts towards the NIR. An N molar concentration of ~0.8% corresponds to E_+ and E_- values of 1.8 eV and 1.27 eV, i.e. approaching the bandgap of Si and $GaAs_{1-x}P_x$ ($x = 0.33$), respectively: noteworthy, the combination of the latter semiconductors in a conventional two-junction tandem (series connected) SC could reach a maximum theoretical PCE of 30% [46]. PCE figures of planar IBSCs based on various III–N–V alloys have been calculated by Cànovas *et al* [47], demonstrating that N concentrations in the 1%–3.5% range would allow efficiencies above 60% under concentrated solar power irradiation.

In a planar III–N–V based IBSC, the dilute nitrides inherent short diffusion lengths (a few tens of nm) of minority charge carriers impose a reduced thickness of the IB absorber layer to achieve good collection efficiencies of photo-generated carriers, while large alloy thicknesses are required for efficient light absorption in the NIR. This trade-off has placed severe limitations on PCE values that could be practically achieved by a planar IBSC based on such materials. In addition, large values of III–N–V epilayer thickness in planar heterostructures deposited on commercially available substrates (GaAs, GaP, Si) may lead to lattice mismatches and elastic strains—in the order of 10^{-3}–10^{-2} (for N content in the III–N–V alloy up to a few percent), which may readily relax resulting in dislocation nucleation [33, 48] or other types of extended defects [49] and deterioration of the materials electronic properties.

The use of dilute nitrides (III–N–V) within a core-multishell nanowire together with the nanowire ability to elastically accommodate the large lattice mismatches associated with III–N–V alloys promises to solve the above-mentioned limitations of planar III–N–V based IBSC devices. Indeed, (i) axially-long nanowire heterostructures, together with proper exploitation of nano-antenna and wave-guiding effects, would allow for the efficient absorption of sub-bandgap photons, while (ii) radial p–n junction

nanowires would permit one to obtain short (in the order of a few tens of nm) photo-generated carrier transit lengths and improved carrier collection efficiencies. Large PCE figures are thus expected for such novel nanowire IBSCs, while still retaining a simpler (radial) single-junction nanowire geometry.

The proposed schematic of a single-nanowire IBSC structure based on a III–N–V compound is shown in figure 2(b): the nanowire is made of a central p^+-doped GaAs core, overgrown by a thin shell of GaNAs alloy. The IB absorber is n-type doped to ensure an efficient TSPA process and sandwiched between an inner p-doped AlGaAs electron blocking barrier and an outer n-doped AlGaAs emitter shell [43]. The latter shells ensure proper electric insulation of the IB GaNAs alloy. The outermost shell is made of an n^+-doped GaAs as an electron collecting contact. An inverted radial structure with, for example, an n^+-GaAs core and an outmost p^+-GaAs contact shell is also possible. Figure 1 shows that the total junction area of an SC made of a dense array of nanowires according to the schematic in figure 2(b) will remain below that of planar IBSCs. It is noteworthy that all interfaces within the proposed IBSC would be grown by the conventional VS process: the number of interface defects and associated electronic states are thus expected to be substantially comparable to those occurring at the analogue interfaces of MBE or MOVPE grown planar III–V tandem SCs, provided that defects within the VLS-grown nanowire core (e.g. stacking faults, twins, etc) or at the core–shell interfaces would not occur/propagate within the device active volume or remain ineffective. In this regard, much remains to be clarified on the role of these and other defects in determining the actual losses of NWSCs, and their possible suppression during nanowire self-assembly.

Finally, the two blocking AlGaAs shells in figure 2(b) would ensure light wave-guiding of the incident sunlight, so as to concentrate solar radiation within the GaNAs shell, although proper conditions for such effects and estimates of actual concentration factors achievable within the nanowire device remain to be determined and will require detailed FDTD simulations. PCEs in excess of those predicted for planar IBSC analogues (potentially up to 2× those calculated for conventional NWSCs) can thus be foreseen for the proposed nanowire IBSCs.

An important figure of merit to evaluate alternative PV technologies is defined by the cost of fabrication of a concentrated PV module (CPM) per generated peak power. A preliminary estimate of this figure employing a conventional NWSC was reported by Gotkas *et al* [29] and showed a significant reduction when compared to CPMs based on conventional III–V tandem SCs, a result essentially due to the smaller volumes (a few percent with respect to planar SCs) of costly III–V materials required for fabricating NWSCs. We point out that the fabrication of the nanowire IBSCs proposed in this work would require about the same amount of materials as for conventional NWSCs but would result in much higher PCEs. The cost per generated watt-peak of present nanowire IBSCs is thus expected to be reduced by 50% (or more) with respect to that of conventional NWSCs, as reported in [29].

4. Technology challenges and perspectives

Despite the large amount of research reported on the MBE and MOVPE epitaxy of planar III–N–V compounds over the last two decades [50], self-assembling of III–N–V based core-(multi)shell nanowires is still in its infancy. A major obstacle to be addressed by these technologies is the large miscibility gap existing between III–N and III–V (arsenides, phosphides) compounds, which makes the incorporation of N atoms into III–V crystals difficult and facilitates the formation of large concentrations of N-related non-radiative recombination (NRR) centers. Non-equilibrium growth conditions must thus be adopted to obtain sufficient levels of N-incorporation into the GaAs matrix; this translates into the need for relatively low growth temperatures, large N overpressures and suitable growth rates.

To date, catalyst-free growth of GaAs–GaNAs core-(multi)shell nanowires has been reported for N plasma-assisted MBE only [51]: N incorporation up to 2% was shown for GaNAs shells grown at around 430 °C, although such very low growth temperature may promote the formation of abundant N-related NRR centers, leading to a decrease of the material internal quantum efficiency. Still, optically pumped lasing from the GaNAs shell of a single GaAs/GaNAs core/shell nanowire was demonstrated below 150 K [52]. In comparison to MBE, much less work has been reported on the self-assembly of III–N–V nanowires by MOVPE [42]. To the best of our knowledge, no reports can be found on the MOVPE growth of GaNAs-based core-(multi)shell nanowires. A problem in the MOVPE of planar and nanowire structures of III–N–V alloys is the right choice of the N-containing molecular precursor. Several N precursors have been employed for the low-temperature ($<$650 °C) growth of dilute nitride III–V compounds; among others, NF_3, hydrazine (N_2H_4), monomethyl-hydrazine (MeN_2H_3), dimethyl-hydrazine ($Me_2N_2H_2$), and tertiary-butyl-hydrazine ($^tBuN_2H_3$) [53]. The latter is the least stable among such N-precursors (its pyrolysis begins at 220 °C and reaches 100% above 350 °C [54]) due to the relatively

weaker tertiarybutyl-N bond; therefore, it leads to improved N-incorporation efficiency at lower temperatures. Our research group has recently demonstrated the Au-catalyzed MOVPE growth of GaAs–GaNAs core–shell nanowires employing $^{t}BuN_2H_3$ for GaNAs shells overgrowth at temperatures around 540 °C–560 °C [55]. However, much work remains to be done in the case of MOVPE.

No attempts to grow a nanowire-based IBSC structure similar to that shown in figure 2(b) have been reported so far, nor any studies on the n-type doping of the IB of GaNAs shells have yet been published. Assessing the structural, functional and electronic parameters of core-multishell nanowires, such as those proposed in figure 2(b) and controlling their growth appears clearly more difficult than for axially-modulated nanowire devices. A combination of high spatial resolution electron tomographic microscopy [56, 57] and spectroscopic [58] characterization methods, supported by a predictive modeling of their radial growth and doping efficiency [23, 42] appears fruitful for future technology development.

In conventional SC structures based on InGaNAs alloys the concentration of N-related defects/traps correlates with the low V_{oc} values of the cell, this being explained by the trap-induced reduction of the material quasi-Fermi level [59], leading to a deterioration of the cell performance. Rapid thermal annealing (RTA) of bulk-like dilute nitride alloys at relatively high (>700 °C) temperatures in N_2/H_2 gas ambient is employed to reduce the fraction of non-substitutional N atoms in the crystal and increase the radiative emission efficiency of III–N–V alloys; RTA has also been proven to be effective for self-catalyzed Ga(N)AsP nanowires and GaAsP/GaNAsP core–shell nanowires grown by MBE [60]. Interestingly, the passivation of N-related NRR centers in GaAs/GaNAs core/shell nanowires was recently claimed by post-growth hydrogenation upon H_2 plasma treatment of MBE-grown nanowires, leading to improved optical properties [61]. This effect is clearly made possible by the nanowire's high surface-to-volume ratios, favoring an almost uniform H incorporation into the nanowire's small volume. In this respect, it is well known that the use of N–H bond-containing precursors leads to the unintentional incorporation of H into III–N materials grown by MOVPE. If this is the case also for III–N–V alloys, it would favor a self-passivation of NRR centers during MOVPE growth.

5. Conclusions

Despite the large research efforts carried out over the last two decades, conventional NWSCs based on III–V compounds do not currently meet the theoretical PCE figures. Still, the inherent advantages of nanowires, i.e. (i) their super-absorptive optical properties, (ii) their ability to elastically accommodate large lattice mismatches and (ii) the reduced material volumes, still make them very attractive for PV applications. In this paper we proposed an innovative approach towards the realization of very high efficiency NWSCs consisting of the implementation of nanowire-based IBSCs, i.e. the combination of the nanowire architecture with the use of IBGSs, namely III–N–V compounds, as the sunlight absorbing material. These nanowire IBSCs would allow multiple-band absorption of the solar spectrum within a single p–n junction nanowire device. Unprecedentedly high PCEs figures (roughly 2× those of conventional NWSCs) may thus be foreseen. A perspective device structure of a GaNAs based single-nanowire IBSC is further proposed and discussed: in contrast to most conventional NWSCs reported so far, the novel device requires a single radial junction and a carefully designed core-multishell nanowire structure. The fabrication of III–N–V based nanowire-IBSCs requires precise control of the N-incorporation (within the 0.8%–1.5% range), doping levels, reduced number of NRR centers, and suitably-designed shell thickness sequences. The potential of, and possible limitations and challenges of using MBE and MOVPE self-assembly technologies for the synthesis of III–N–V based nanowire devices have been discussed. Further research appears to be necessary in the near future to implement and prove the PV effectiveness of the proposed III–N–V based nanowire IBSCs.

Data availability statement

No new data were created or analysed in this study.

Acknowledgment

The authors would like to acknowledge funding from the Ministry for University and Research (MUR) of Italy and Next Generation EU through the PRIN 2022 PNRR Project P2022B9P9H (‘*SOLNANO*’).

Author contributions

Paola Prete 0000-0002-4948-4718
Conceptualization (equal), Investigation (equal), Supervision (lead), Writing – original draft (equal), Writing – review & editing (equal)

Nico Lovergine 0000-0003-0190-4899
Conceptualization (equal), Funding acquisition (lead), Visualization (equal), Writing – original draft (equal), Writing – review & editing (equal)

References

[1] Spillias S, Kareiva P, Ruckelshaus M and McDonald-Madden E 2020 Renewable energy targets may undermine their sustainability *Nat. Clim. Change* **10** 974

[2] Rosa W 2017 "Transforming our world: the 2030 agenda for sustainable development" *A New Era in Global Health* ed W Rosa (Springer) 529–67

[3] Barbato M *et al* 2021 CdTe solar cells: technology, operation and reliability *J. Appl. Phys.* **54** 333002

[4] Friedlmeier T M, Jackson P, Bauer A, Hariskos D, Kiowski O, Menner R, Wuerz R and Powalla M 2017 High-efficiency Cu(In,Ga)Se_2 solar cells *Thin Solid Films* **633** 13

[5] NREL, Best research-cell efficiency chart (available at: www.nrel.gov/pv/cell-efficiency.html)

[6] Shockley W and Queisser H J 1961 Detailed balance limit of efficiency of p-n junction solar cells *J. Appl. Phys.* **32** 510

[7] Lopes T S *et al* 2023 Cu(In,Ga)Se_2 based ultrathin solar cells the pathway from lab rigid to large scale flexible technology *npj Flex. Electron.* **7** 4

[8] Anctil A *et al* 2023 Status report on emerging photovoltaics *J. Photon. Energy* **13** 042301

[9] Mayer B, Janker L, Rudolph D, Loitsch B, Kostenbader T, Abstreiter G, Koblmüller G and Finley J J 2016 Continuous wave lasing from individual GaAs-AlGaAs core-shell nanowires *Appl. Phys. Lett.* **108** 071107

[10] Parkinson P, Alanis J A, Peng K, Saxena D, Mokkapati S, Jiang N, Fu L, Tan H H and Jagadish C 2018 Modal refractive index measurement in nanowire lasers—a correlative approach *Nano Futures* **2** 035004

[11] Gallo E M, Chen G, Currie M, McGuckin T, Prete P, Lovergine N, Nabet B and Spanier J E 2011 Picosecond response times in GaAs/AlGaAs core/shell nanowire-based photodetectors *Appl. Phys. Lett.* **98** 241113

[12] Chen G, Sun G, Ding Y J, Prete P, Miccoli I, Lovergine N, Shtrikman H, Kung P, Livneh T and Spanier J E 2013 Direct measurement of band edge discontinuity in individual core-shell nanowires by photocurrent spectroscopy *Nano Lett.* **13** 4152

[13] Persano A, Nabet B, Taurino A, Prete P, Lovergine N and Cola A 2011 Polarization anisotropy of individual core/shell GaAs/AlGaAs nanowires by photocurrent spectroscopy *Appl. Phys. Lett.* **98** 153106

[14] Chen G, Gallo E M, Leaffer O D, McGuckin T, Prete P, Lovergine N and Spanier J E 2011 Tunable hot-electron transfer within a single core-shell nanowire *Phys. Rev. Lett.* **107** 156802

[15] Al-Abri R, Choi H and Parkinson P 2021 Measuring, controlling and exploiting heterogeneity in optoelectronic nanowires *J. Phys. Photon.* **3** 022004

[16] Czaban J A, Thompson D A and LaPierre R R 2009 GaAs core-shell nanowires for photovoltaic applications *Nano Lett.* **9** 148

[17] Goto H, Nosaki K, Tomioka K, Hara S, Hiruma K, Motohisa J and Fukui T 2009 Growth of core–shell InP nanowires for photovoltaic application by selective-area metal organic vapor phase epitaxy *Appl. Phys. Express* **2** 035004

[18] Wagner R S and Ellis W C 1964 Vapor-liquid-solid mechanism of single crystal growth *Appl. Phys. Lett.* **4** 89

[19] Paiano P, Prete P, Speiser E, Lovergine N, Richter W, Tapfer L and Mancini A M 2007 GaAs nanowires grown by Au-catalyst-assisted MOVPE using tertiarybutylarsine as group-V precursor *J. Cryst. Growth* **298** 620

[20] Miccoli I, Prete P, Marzo F, Cannoletta D and Lovergine N 2011 Synthesis of vertically-aligned GaAs nanowires on GaAs/(111)Si hetero-substrates by metalorganic vapour phase epitaxy *Cryst. Res. Technol.* **46** 795

[21] Chen G, Gallo E M, Burger J, Nabet B, Cola A, Prete P, Lovergine N and Spanier J E 2010 On direct- writing methods for electrically contacting GaAs and Ge nanowire devices *Appl. Phys. Lett.* **96** 223107

[22] Wallentin J and Borgström M T 2011 Doping of semiconductor nanowires *J. Mater. Res.* **26** 2142 and references therein

[23] Miccoli I, Prete P and Lovergine N 2015 Mass-transport driven growth dynamics of AlGaAs shells deposited around dense GaAs nanowires by metalorganic vapor phase epitaxy *CrystEngComm* **17** 5998

[24] Yoshimura M, Nakai E, Tomioka K and Fukui T 2013 Indium phosphide core–shell nanowire array solar cells with lattice-mismatched window layer *Appl. Phys. Express* **3** 05230

[25] Åberg I *et al* 2016 A GaAs nanowire array solar cell with 15.3% efficiency at 1 Sun *IEEE J. Photovolt.* **6** 185

[26] Mariani G, Scofield A C, Hung C-H and Huffaker D L 2013 GaAs nanopillar-array solar cells employing *in situ* surface passivation *Nat. Commun.* **4** 1497

[27] Li Z, Tan H H, Jagadish C and Fu L 2018 III–V semiconductor single nanowire solar cells: a review *Adv. Mater. Technol.* **3** 1800005

[28] Wen L, Zhao Z, Li X, Shen Y, Guo H and Wang Y 2011 Theoretical analysis and modeling of light trapping in high efficiency GaAs nanowire array solar cells *Appl. Phys. Lett.* **99** 143116

[29] Goktas N I, Wilson P, Ghukasyan A, Wagner D, McNamee S and LaPierre R R 2018 Nanowires for energy: a review *Appl. Phys. Rev.* **5** 041305

[30] Wang S, Yan X, Zhang X, Li J and Ren X 2015 Axially connected nanowire core-shell p-n junctions: a composite structure for high-efficiency solar cells *Nanoscale Res. Lett.* **10** 22

[31] Alcer D, Tirrito M, Hrachowina L and Borgström M T 2024 Vertically processed GaInP/InP tandem-junction nanowire solar cells *ACS Appl. Nano Mater.* **7** 2352

[32] Yao M, Cong S, Arab S, Huang N, Povinelli M L, Cronin S B, Dapkus P D and Zhou C 2015 Tandem solar cells using GaAs nanowires on Si: design, fabrication, and observation of voltage addition *Nano Lett.* **15** 7217

[33] Prete P, Calabriso D, Burresi E, Tapfer L and Lovergine N 2023 Lattice strain relaxation and compositional control in As-rich GaAsP/(100)GaAs heterostructures grown by MOVPE *Materials* **16** 4254

[34] Limpert S *et al* 2017 Single-nanowire, low-bandgap hot carrier solar cells with tunable open-circuit voltage *Nanotechnology* **24** 434001

[35] Esmaielpour H, Isaev N, Makhfudz I, Döblinger M, Finley J J and Koblmüller G 2024 Strong dimensional and structural dependencies of hot carrier effects in InGaAs nanowires: implications for photovoltaic solar cells *ACS Appl. Nano Mater.* **7** 2817
[36] Krogstrup P, Jørgensen H I, Heiss M, Demichel O, Holm J V, Aagesen M, Nygård J and Fontcuberta i Morral A 2013 A Single-nanowire solar cells beyond the Shockley–Queisser limit *Nat. Photon.* **7** 306
[37] Cretì A, Prete P, Lovergine N and Lomascolo M 2022 Enhanced optical absorption of GaAs near-band-edge transitions in GaAs/AlGaAs core-shell nanowires: implications for nanowire solar cells *ACS Appl. Nano Mater.* **5** 18149
[38] Mayer B *et al* 2013 Lasing from individual GaAs-AlGaAs core-shell nanowires up to room temperature *Nat. Commun.* **4** 2931
[39] Gu Z, Prete P, Lovergine N and Nabet B 2011 On optical properties of GaAs/AlGaAs core-shell periodic nanowire arrays *J. Appl. Phys.* **109** 064314
[40] Anttu N 2015 Shockley–Queisser detailed balance efficiency limit for nanowire solar cells *ACS Photonics* **2** 446
[41] Mokkapati S and Jagadish C 2016 Review on photonic properties of nanowires for photovoltaics *Opt. Express* **24** 17345
[42] Prete P and Lovergine N 2020 Dilute nitride III–V nanowires for high efficiency intermediate-band photovoltaic cells: materials requirements, self-assembly methods and properties *Prog. Cryst. Growth Charact. Mater.* **66** 100510
[43] Luque A and Martí A 1997 Increasing the efficiency of ideal solar cells by photon induced transitions at intermediate levels *Phys. Rev. Lett.* **78** 5014
[44] Ahsan N, Miyashita N, Islam M M, Yu K M, Walukiewicz W and Okada Y 2012 Two- photon excitation in an intermediate band solar cell structure *Appl. Phys. Lett.* **100** 172111
[45] Hossain M F, Yagi S and Yaguchi H 2025 Effects of carrier supply to the intermediate band by impurity doping on two-step photocurrent generation in GaAs:N-Based intermediate band solar cell *North Am. Acad. Res.* **8** 112
[46] White T P, Lal N N and Catchpole K R 2014 Tandem solar cells based on high-efficiency c-Si bottom cells: top cell requirements for $>30\%$ efficiency *IEEE J. Photovolt.* **4** 208
[47] Cànovas E, Martí A, Luque A and Walukiewicz W 2008 Optimum nitride concentration in multiband III-N-V alloys for high efficiency ideal solar cells *Appl. Phys. Lett.* **93** 174100
[48] Lovergine N, Liaci L, Ganière J-D, Leo G, Drigo A V, Romanato F, Mancini A M and Vasanelli L 1995 Inhomogeneous strain relaxation and defect distribution of ZnTe epilayers deposited on (100)GaAs by metalorganic vapor phase epitaxy *J. Appl. Phys.* **78** 229
[49] Lovergine N, Miccoli I, Tapfer L and Prete P 2023 GaAs hetero-epitaxial layers grown by MOVPE on exactly-oriented and off-cut (111)Si: lattice tilt, mosaicity and defects content *Appl. Surf. Sci.* **634** 157627
[50] Erol A 2008 *Dilute III–V Nitride Semiconductors and Material Systems: Physics and Technology* 1st edn ed A Erol (Springer) (https://doi.org/10.1007/978-3-540-74529-7)
[51] Yukimune M, Fujiwara R, Ikeda H, Yano K, Takada K, Jansson M, Chen W M, Buyanova I A and Ishikawa F 2018 GaAs/GaNAs core-multishell nanowires with nitrogen composition exceeding 2% *Appl. Phys. Lett.* **113** 011901
[52] Chen S, Jansson M, Stehr J E, Huang Y, Ishikawa F, Chen W M and Buyanova I A 2017 Dilute nitride nanowire lasers based on a GaAs/GaNAs core/shell structure *Nano Lett.* **17** 1775
[53] Ptak A J, Kurtz S, Curtis C, Reedy R and Olson J M 2002 Incorporation effects in MOCVD-grown (In)GaAsN using different nitrogen precursors *J. Cryst. Growth* **243** 231
[54] Pohl U, Möller C, Knorr K, Richter W, Gottfriedsen J, Schumann H, Rademann K and Fielicke A 1999 Tertiarybutylhydrazine: a new precursor for the MOVPE of group III-nitrides *Mater. Sci. Eng. B* **59** 20
[55] Garzia L, Prete P, Burresi E, Tapfer L and Lovergine N 2025 in preparation
[56] Lubk A, Wolf D, Prete P, Lovergine N, Niermann T, Sturm S and Lichte H 2014 Nanometer-scale tomographic reconstruction of three-dimensional electrostatic potentials in GaAs/AlGaAs core-shell nanowires *Phys. Rev. B* **90** 125404
[57] Wolf D, Hubner R, Niermann T, Sturm S, Prete P, Lovergine N, Buchner B and Lubk A 2018 Three-dimensional composition and electric potential mapping of III−V core−multishell nanowires by correlative STEM and holographic tomography *Nano Lett.* **18** 4777
[58] Prete P, Wolf D, Marzo F and Lovergine N 2019 Nanoscale spectroscopic imaging of GaAs-AlGaAs quantum well tube nanowires: correlating luminescence with nanowire size and inner multishell structure *Nanophotonics* **8** 1567
[59] Kurtz S *et al* 2005 Understanding the potential and limitations of dilute nitride alloys for solar cells *NREL Report no. NREL/CP-520-38998* (available at: www.nrel.gov/docs/fy06osti/38998.pdf)
[60] La R, Pan J L, Bastiman F and Tu C W 2016 Self-catalyzed Ga(N)AsP nanowires and GaAsP/GaNAsP core-shell nanowires grown on Si (111) by gas-source molecular beam epitaxy *J. Vac. Sci. Technol. B* **34** 02L108
[61] Jansson M, Nosenko V V, Hemmingsson C, Pozina G, Ishikawa F, Chen W M and Buyanova I A 2025 Passivation of localized states in GaAs/GaNAs core/shell nanowires by post-growth hydrogenation *J. Appl. Phys.* **137** 205703